

Thermal expansion of single-crystalline $\text{La}_{0.83}\text{Sr}_{0.17}\text{MnO}_3$: The importance of temperature-induced strain for the electrical resistivity

J. J. Neumeier

*Department of Physics, Florida Atlantic University, Boca Raton, Florida 33431
and Walther-Meissner-Institut für Tieftemperaturforschung, Walther-Meissner-Strasse 8, D-85748 Garching, Germany*

K. Andres

Walther-Meissner-Institut für Tieftemperaturforschung, Walther-Meissner-Strasse 8, D-85748 Garching, Germany

K. J. McClellan

*Materials Science and Technology Division, Los Alamos National Laboratory, Los Alamos, New Mexico 87545
(Received 4 August 1998)*

Thermal expansion, magnetization, and electrical-resistivity measurements of single crystalline $\text{La}_{0.83}\text{Sr}_{0.17}\text{MnO}_3$ are presented. A first-order structural transition occurs at 300 K, transforming the high-temperature rhombohedral phase into an orthorhombic phase. The paramagnetic to ferromagnetic phase transition is second order and is clearly revealed as a change in slope of the linear-thermal expansion $\Delta l/l$ at $T_c = 265$ K. The temperature derivative of $\Delta l/l$ yields the thermal-expansion coefficient α ; thermodynamic analysis of α near T_c reveals isotropic-uniaxial pressure derivatives of T_c . Strain arising from the structural and magnetic transitions is shown to influence the electrical resistivity. [S0163-1829(99)01103-0]

The electrical properties of nearly metallic manganese perovskites such as the title compound $\text{La}_{0.83}\text{Sr}_{0.17}\text{MnO}_3$ are closely intertwined with crystallographic distortions and magnetic behavior. Chemical substitution¹ yields a wide range of ferromagnetic-transition temperatures and $\rho(T)$ behavior, where ρ is the electrical resistivity and T is the temperature. Further control of the physical properties is possible through thin-film deposition techniques,² which can capitalize on large strain^{3,4} effects. An exceptionally large magnetoresistance occurs and is referred to as colossal magnetoresistance (CMR). Although early theoretical considerations clarified the electrical-transport properties within the framework of the double-exchange (DE) model, more recent research reveals the importance of the Jahn-Teller distortion in the MnO_6 octahedra, which is synonymous with the formation of lattice polarons through a strong electron-phonon interaction.⁵ This physical picture has similarities to polaronic models for EuO .⁶ The unusual sensitivity to strain (including strain induced by hydrostatic pressure) is likely a result of the Jahn-Teller distortion's sensitivity to strain. A number of local-structural studies have observed the Jahn-Teller distortion,⁷ and a recent x-ray-absorption fine-structure investigation has provided a direct relation between MnO_6 distortions and the magnetic properties.⁸ The Jahn-Teller distortion is reduced as T is lowered below the ferromagnetic Curie temperature T_c , reflecting a decrease in coupling between the electronic and vibrational states.⁸ The most compelling experimental observation regarding an electron-phonon interaction and its importance for the magnetic properties is the strong oxygen isotope effect on T_c in $\text{La}_{1-x}\text{Ca}_x\text{MnO}_3$,⁹ whereby specimens with the heavier oxygen isotope ^{18}O exhibit lower T_c values.

A handful of experimental studies have reported results of thermal-expansion measurements on polycrystalline speci-

mens. Ibarra *et al.* measured linear-thermal expansion $\Delta l/l$ using a strain-gauge technique,¹⁰ which unveiled a large anomaly in the thermal-expansion coefficient α at T_c and some other features that were attributed to polarons. Measurements under hydrostatic pressure¹¹ showed that the anomaly in α and the peak in the electrical resistivity at T_c were rapidly reduced by pressure, thus indicating the importance of the unit-cell volume for the electrical properties. Measurements of $\Delta l/l$ and the influence of pressure on the electrical resistivity of insulating and metallic $\text{La}_{0.79}\text{Ca}_{0.21}\text{MnO}_{3+y}$ specimens¹² further illustrate the importance of unit-cell volume in determining the electrical properties, and ultimately the CMR effect. Another study indicates the electron-phonon interaction's significance for the thermal expansion.¹³

The close physical connection between thermal expansion ($\partial V/\partial T$) and pressure (or strain) is provided by the Ehrenfest relation,¹⁴ which will be discussed in detail below. Since pressure is known to strongly influence T_c , thermal-expansion measurements provide an alternative method for investigating the unusually large effect of pressure on T_c in manganese oxides.^{4,10-12} Herein the first linear-thermal expansion measurements of a single-crystal CMR material are presented; the ferromagnetic $\text{La}_{0.83}\text{Sr}_{0.17}\text{MnO}_3$ specimen was measured with high-resolution capacitive dilatometry. This composition is known to exhibit a rhombohedral to orthorhombic phase transition above T_c ,¹⁵ which is sensitive to the magnetic field; it is also near the compositional antiferromagnetic-ferromagnetic phase boundary.¹⁶

A single crystal of $\text{La}_{0.83}\text{Sr}_{0.17}\text{MnO}_3$ was grown in air from sintered polycrystalline rods of the same stoichiometry. The polycrystalline rods were prepared as described previously.¹² The tips of the feed and seed rods were melted and joined in an optical image furnace. The rods were rotated

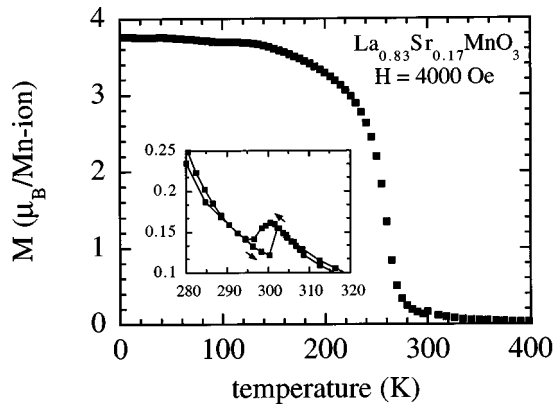


FIG. 1. Magnetization vs temperature at 4000 Oe. In the inset, the region near 300 K is enlarged; the arrows indicate cooling and warming.

in opposite directions at 50 rpm and fed through the hot zone at 3–5 mm/h. A piece of the resulting crystal was examined by powder x-ray diffraction and found to be single phase; electron-microscope analysis confirmed the stoichiometry. Another piece with dimensions of $1.78 \times 1.36 \times 1.19 \text{ mm}^3$ was oriented using Laue diffraction. The a , b , and c axes discussed below refer to the orthorhombic axes. The magnetic measurements were conducted with a commercially available magnetometer. Thermal expansion measurements utilized a capacitive dilatometer constructed entirely of high-purity quartz.¹⁷ The small-thermal expansion of quartz results in a minor correction for the cell's contribution to the observed-length change of the specimen (about 2% of the specimen-length change); this device can resolve a length change in a 1-mm-long specimen of 0.1 Å.

In Fig. 1 the magnetization in units of $\mu_B/\text{Mn ion}$ (where μ_B is the Bohr magneton) is plotted vs T at 4000 Oe. The specimen becomes ferromagnetic below $T_c = 265 \text{ K}$ with a saturation moment of $M(5 \text{ K}, 4000 \text{ Oe}) = 3.8 \mu_B/\text{Mn ion}$; T_c is determined from the low-field data in Fig. 2. Near room temperature, a small feature in $M(T)$ is apparent. This region is enlarged in the inset of Fig. 1 where measurements taken upon cooling and warming are displayed. These data indicate that the transition is hysteretic; we note, however, that the magnetometer undershoots the set temperature in the cool-down mode so the amount of hysteresis indicated in the figure is not accurate. A small dip in the $M(T)$ data of Fig. 1 is

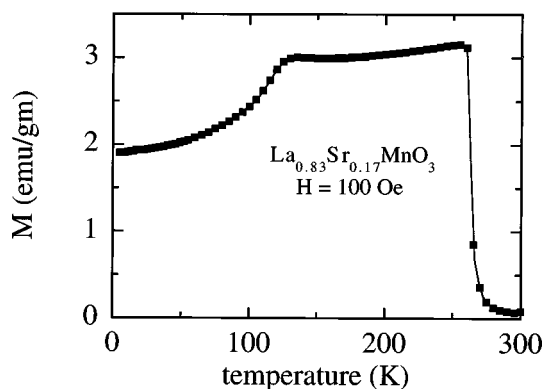


FIG. 2. Magnetization vs temperature at 100 Oe illustrating the feature at 128 K due to spin canting.

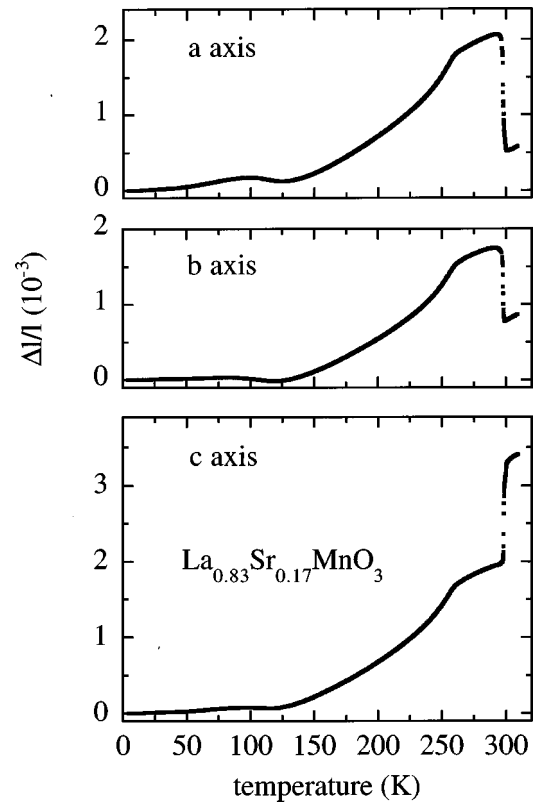


FIG. 3. The linear thermal expansion $\Delta l/l$ vs temperature for the three orthorhombic axes. The structural phase transition from rhombohedral to orthorhombic occurs at 300 K and is a first-order transition. The paramagnetic to ferromagnetic transition occurs at 265 K and is second order as indicated by the continuous change in slope of $\Delta l/l$.

visible near 128 K. This region is clarified in Fig. 2, which displays $M(T)$ data taken at 100 Oe where a clear decrease in M is observed at 128 K. This is a second magnetic transition where the Mn magnetic moments cant antiferromagnetically. Increasing the magnetic field destroys this canting, thus only a weak feature is apparent in the data of Fig. 1, which were taken at 4000 Oe.

The linear-thermal expansion $\Delta l/l$ is illustrated in Fig. 3 for the three orthorhombic axes. All plots in Fig. 3 employ the same vertical scale. As the specimen is cooled below 300 K, an expansion is observed in the a and b directions and contraction occurs along the c direction. The discontinuous change in $\Delta l/l$ is indicative of a first-order transition, in accordance with our observation of hysteresis. The general features of these results are in agreement with a crystallographic study by Asamitsu *et al.*,¹⁵ although the temperature of the structural transition is about 10 K higher for our crystal, and the length changes in Fig. 3 correspond to slightly different lattice-parameter changes. These discrepancies probably result from slight compositional differences between the two specimens. The overall volume change associated with the structural transition is $\Delta V/V = 1.31 \times 10^{-3}$ compared with 2.61×10^{-3} observed by Asamitsu *et al.*¹⁵

The data of Fig. 3 illustrate that a sharp change in the slope of $\Delta l/l$ occurs at T_c . The slope change is well defined and continuous, thereby characterizing the paramagnetic to ferromagnetic phase transition as second order in nature. The slope changes again at 128 K, corresponding to the tempera-

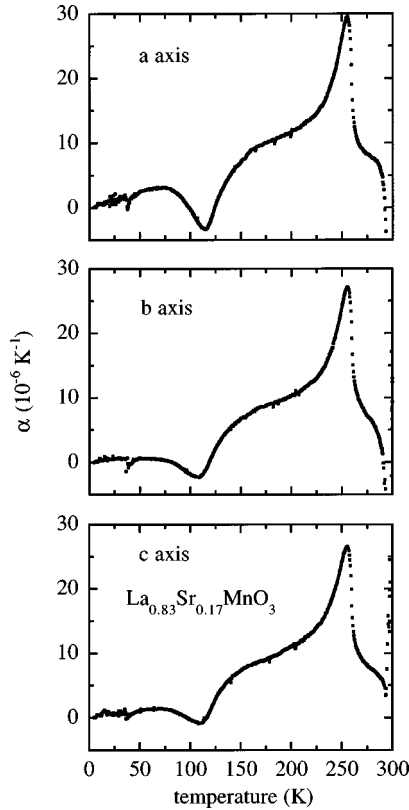


FIG. 4. Thermal-expansion coefficient α vs temperature for the three orthorhombic axes. Data are shown for temperatures below the structural transition.

ture where antiferromagnetic canting occurs; this slope change is also continuous and indicative of a second-order phase transition. Thus, the linear-thermal expansion data of Fig. 3 reveal three distinct phase transitions in this specimen.

The thermal-expansion coefficient α was determined by taking a point-to-point temperature derivative of the data in Fig. 3, the spacing of which are 0.5 K. The resulting data are plotted in Fig. 4 for the temperature range *below* the structural transition using the same vertical scale in all three panels of the figure. At T_c a jump in α occurs. Plotting the data near T_c on one plot for all three crystallographic axes (not shown) illustrates that the jumps at T_c are of equal magnitude for the three axes. Thus, the transition into the ferromagnetic state results in an isotropic change in the rate of lattice contraction. At the antiferromagnetic transition near 128 K the thermal expansion displays a peak for all three crystallographic directions. The peak exhibited for the *a* direction is slightly larger than for the *b* and *c* directions, indicating a slight anisotropy; however, no anisotropy was observed in the low-field magnetic-susceptibility measurements. Another small feature is observed in α near 35 K for all three crystallographic directions; this feature is, however, an artifact of the background subtraction.

The volume-thermal expansion coefficient β is obtained by adding the linear-thermal expansion coefficients for the three crystallographic axes. The jump in the volume-thermal expansion coefficient $\Delta\beta$ at T_c is related to the pressure dependence of T_c near $P=0$, dT_c/dP , through the Ehrenfest relation for a second-order phase transition, which is given by

$$\Delta\beta = \frac{\Delta C_p}{V_{\text{mol}} T_c} \left[\frac{dT_c}{dP} \right]. \quad (1)$$

In Eq. (1), ΔC_p is the jump in the constant pressure specific heat at T_c and V_{mol} is the molar volume. Equation (1) is obtained by considering the continuity of the Gibb's free energy in constant magnetic field at T_c .¹⁴ In a system that possesses anisotropy in α , Eq. (1) can be rewritten as

$$\Delta\alpha_i = \frac{\Delta C_p}{V_{\text{mol}} T_c} \left[\frac{dT_c}{d\sigma_i} \right], \quad (2)$$

where $\Delta\alpha_i$ is the jump in the linear-thermal expansion coefficient in the *i*th crystallographic direction ($i = a, b, \text{ or } c$) and $dT_c/d\sigma_i$ is the uniaxial-pressure derivative in that direction. Equation (2) has successfully been used to obtain the uniaxial-pressure derivatives of the superconducting transition temperature in a number of highly anisotropic copper oxide^{17,18} and organic superconductors.^{17,19} Consideration of Eq. (2) and the data in Fig. 4 indicates that the three uniaxial pressure derivatives are identical for $\text{La}_{0.83}\text{Sr}_{0.17}\text{MnO}_3$. To our knowledge, this is the first paper to reveal the influence of pressure on T_c in the ABO_3 CMR oxides to be isotropic.

Equation (1) can be used to estimate the pressure derivative dT_c/dP if ΔC_p is known. To our knowledge, no measurements of ΔC_p exist in the literature for this exact composition. Volger²⁰ reported a value of $\Delta C_p = 16.7$ J/mol K for $\text{La}_{0.7}\text{Sr}_{0.3}\text{MnO}_3$ with $T_c = 340$ K. Measurements on a specimen of $\text{La}_{0.7}\text{Ca}_{0.3}\text{MnO}_3$ revealed a value of $\Delta C_p = 48.6$ J/mol K.²¹ Using the values of $\Delta C_p = 16.7$ J/mol K, $V_{\text{mol}} = 3.57 \times 10^{-5}$ m³/mol and the observed jump of $\Delta\beta = 62 \times 10^{-6}$ K⁻¹ we calculate $dT_c/dP = 35$ K/GPa via Eq. (1). A value of $dT_c/dP = 11$ K/GPa (Ref. 22) was reported for a specimen of $\text{La}_{0.825}\text{Sr}_{0.175}\text{MnO}_3$. Noting the strong compositional dependence of dT_c/dP (Refs. 4 and 22) and the fact that $dT_c/dP > 40$ K/GPa has been observed in similar manganese oxides,⁴ we find this value to be reasonable, especially given our uncertainty in ΔC_p . We emphasize that a jump in α near T_c is expected within the framework of thermodynamics of second-order phase transitions and note that similar features are observed in elemental ferromagnets.²³ On a microscopic level, the Bethe curve,²³ which relates the ferromagnetic-interaction energy to volume, predicts a change in this energy as a result of a volume expansion or contraction. As a material passes through its Curie temperature, the change in slope of $\Delta V/V$ is the reciprocal effect.

To put our measurements into perspective, let us consider the thermal expansion of a simple metal. The volume of copper exhibits an expansion,²⁴ when warmed from 4 to 300 K of about 9.6×10^{-3} , nearly a factor of 2 larger than what we observe for our specimen in the range $5 \text{ K} < T < 280 \text{ K}$. The bulk modulus $B_M = -V(dP/dV)$ of copper is 137 GPa,²⁵ while B_M of $\text{La}_{0.83}\text{Sr}_{0.17}\text{MnO}_3$ (Ref. 26) is 182 GPa for temperatures above the structural transition, and in the range 130–140 GPa for temperatures below the structural transition. Although the temperature-dependent volume contraction is weaker than that of a simple metal, and the bulk modulus is comparable (near and below T_c), the influence of pressure on the magnetic and electrical properties of the manganese oxides is radically large^{4,11,12,22} in comparison to

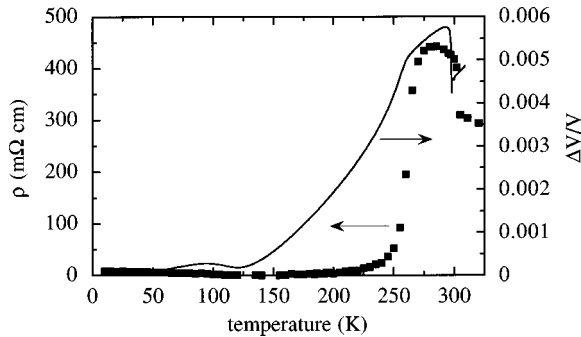


FIG. 5. Electrical resistivity ρ (left abscissa, symbols) and volume-thermal expansion $\Delta V/V$ (right abscissa, solid line) vs temperature.

a simple metal. Thus, temperature-dependent changes in the volume may provide sufficient strain to influence the electrical properties of CMR materials as has been shown by considering specimens near the ferromagnetic-insulating/ferromagnetic-metallic phase boundary.¹²

A number of ABO_3 ferromagnetic CMR specimens exhibit insulating behavior well below T_c ,^{7,12,27,30} this is counter to the DE picture, which requires electron mobility to mediate the ferromagnetic exchange.⁵ However, if the volume-thermal expansion of these specimens is carefully considered, a strong decrease in $\Delta V/V$ below T_c appears to be a signature of metallicity.^{7,12,27,30} Furthermore, a reduction of volume through the application of pressure can induce metallicity in the insulators.^{1,12} Whether the strain induced by the volume contraction below T_c is large enough to influence the electrical resistivity can be examined by defining a term called self-pressure. The self-pressure corresponds to the pressure (at constant temperature), which would be required to realize a change in volume similar to $\Delta V/V$ observed in a given temperature interval. The concept of self-pressure has been previously applied to high-temperature superconductors³¹ and (INVAR) alloys,³² the electrical resistivity of which are also rather sensitive to pressure, albeit significantly less sensitive than that of CMR compounds.

The volume expansion $\Delta V/V$ is plotted in Fig. 5. As the specimen is cooled through the structural transition, $\Delta V/V$ increases by 1.31×10^{-3} . Multiplication of this value by the bulk modulus of 182 GPa provides the negative self-pressure of magnitude 0.24 GPa. Below T_c the volume decreases by 2.59×10^{-3} on cooling from T_c to 220 K; using the bulk modulus of 137 GPa, a positive self-pressure of 0.35 GPa, is obtained. These are substantial pressures for CMR materials and would be expected to strongly alter ρ .^{11,12,22} A plot of the

electrical resistivity versus temperature is displayed in Fig. 5; ρ is isotropic in this sample. At the structural transition a sharp increase in ρ occurs on cooling, corresponding to the volume expansion (and negative self-pressure). At the ferromagnetic transition a drop in ρ occurs corresponding to the volume contraction (and positive self-pressure). Thus, the results presented herein indicate that the self-pressure, or strain, induced by the structural and magnetic transition in this CMR material are large enough to influence the electrical resistivity.

Structural investigations of specimens, which exhibit a metal-insulator transition have revealed^{7,8,27,28} the Jahn-Teller distortion in the MnO_6 octahedral to be reduced as the temperature is lowered below T_c . The MnO_6 distortions can be directly related to the electrical transport properties.^{8,29,33} The data of Figs. 3 and 5 illustrate a stronger contraction in the specimen length and $\Delta V/V$ as T is lowered below T_c . This occurs because of the thermodynamic phase transition into the ferromagnetic state and provides the strain required to reduce the Jahn-Teller distortion and electron-phonon coupling, which, in turn, increases the mobility of the electrons in the e_g levels. These observations suggest that the strain sensitivity of the Jahn-Teller distortion through self-pressure is responsible for the increase in ρ at the structural transition and subsequent decrease in ρ below T_c .

In conclusion, we have presented results of thermal-expansion measurements on single crystalline $La_{0.83}Sr_{0.17}MnO_3$. Our thermodynamic analysis of the second-order paramagnetic to ferromagnetic phase transition indicates that a large-pressure derivative of T_c is expected, in agreement with observations. This analysis also illustrates that the pressure effect on T_c is isotropic. Furthermore, consideration of self-pressure effects suggests that the strain induced as a result of structural and magnetic transitions can influence the temperature dependence of the electrical resistivity through the Jahn-Teller distortion's sensitivity to strain.

ACKNOWLEDGMENTS

J.J.N. and K.A. thank NATO for providing a Collaborative Research Grant No. CRG 970260. J.J.N. is indebted to Florida Atlantic University for a Research Initiation Award and the Walther Meissner Institut for financial support. The authors thank Dr. Michael Kund for assistance with the thermal-expansion measurements and G. Görblich for electron-microscopy investigations. Work at Los Alamos was conducted under the auspices of the U.S. DOE.

¹H. Y. Hwang, S.-W. Cheong, P. G. Radelli, M. Marezio, and B. Batlogg, Phys. Rev. Lett. **75**, 914 (1995); H. Y. Hwang, T. T. M. Palstra, S.-W. Cheong, and B. Batlogg, Phys. Rev. B **52**, 15 046 (1995).

²See, for example, *Science and Technology of Magnetic Oxides*, edited by M. F. Hundley, J. Nickel, R. Ramesh, and Y. Tokura, MRS Symposia Proceedings No. 494 (Materials Research Society, Pittsburgh, 1998).

³Y. Suzuki, H. Y. Hwang, S.-W. Cheong, R. B. Van Dover, A.

Asamitsu, and Y. Tokura, in *Science and Technology of Magnetic Oxides* (Ref. 2), p. 41.

⁴J. J. Neumeier, M. F. Hundley, J. D. Thompson, and R. H. Heffner, Phys. Rev. B **52**, R7006 (1995).

⁵A. J. Millis, B. I. Shraiman, and R. Mueller, Phys. Rev. Lett. **77**, 175 (1996); A. J. Millis, Phys. Rev. B **53**, 8434 (1996).

⁶D. Emin, M. S. Hillary, and N.-L. H. Liu, Phys. Rev. B **35**, 641 (1987).

⁷S. J. L. Billinge, R. G. DiFrancesco, G. H. Kwei, J. J. Neumeier,

- and J. D. Thompson, Phys. Rev. Lett. **77**, 715 (1996); T. A. Tyson, J. Mustre de Leon, S. D. Conradson, A. R. Bishop, J. J. Neumeier, H. Roder, and Jun Zang, Phys. Rev. B **53**, 13 985 (1996).
- ⁸C. H. Booth, F. Bridges, G. H. Kwei, J. M. Lawrence, A. L. Cornelius, and J. J. Neumeier, Phys. Rev. Lett. **80**, 853 (1998).
- ⁹G.-M. Zhao, K. Conder, H. Keller, and K. A. Müller, Nature (London) **381**, 676 (1996).
- ¹⁰M. R. Ibarra, P. A. Algarabel, C. Marquina, J. Blasco, and J. García, Phys. Rev. Lett. **75**, 3541 (1995).
- ¹¹Z. Arnold, K. Kamenev, M. R. Ibarra, P. A. Algarabel, C. Marquina, J. Blasco, and J. García, Appl. Phys. Lett. **67**, 2875 (1995).
- ¹²J. J. Neumeier, A. L. Cornelius, M. F. Hundley, K. Andres, and K. J. McClellan, in *Science and Technology of Magnetic Oxides* (Ref. 2), p. 293.
- ¹³G.-M. Zhao, M. B. Hunt, and H. Keller, Phys. Rev. Lett. **78**, 955 (1997).
- ¹⁴P. Ehrenfest, Communications Leiden **20** (1993).
- ¹⁵A. Asamitsu, Y. Moritomo, Y. Tomioka, T. Arima, and Y. Tokura, Nature (London) **373**, 407 (1995).
- ¹⁶H. Kawano, R. Kajimoto, M. Kubota, and H. Yoshizawa, Phys. Rev. B **53**, 2202 (1996).
- ¹⁷M. Kund, *Uniaxiale Effekte in Organischen und Keramischen Supraleiter* (Hari Deutsch, Reihe Physik, Frankfurt am Main, 1995).
- ¹⁸M. Kund, J. J. Neumeier, K. Andres, J. Markl, and G. Saemann-Ischenko, Physica C **296**, 173 (1998), and references therein.
- ¹⁹M. Kund, J. Lehrke, W. Biberacher, A. Lerf, and K. Andres, Synth. Met. **70**, 949 (1995); M. Kund, H. Müller, N. D. Kushch, K. Andres, and G. Saito, *ibid.* **70**, 951 (1995).
- ²⁰J. Volger, Physica **20**, 49 (1954).
- ²¹A. P. Ramirez, P. Schiffer, S.-W. Cheong, C. H. Chen, W. Bao, T. T. M. Palstra, P. L. Gammel, D. J. Bishop, and B. Zegarski, Phys. Rev. Lett. **76**, 3188 (1996).
- ²²Y. Moritomo, A. Asamitsu, and Y. Tokura, Phys. Rev. B **51**, 16 491 (1995).
- ²³See, for example, E. Kneller, *Ferromagnetismus* (Springer-Verlag, Berlin, 1962), p. 225; Bozorth, *Ferromagnetism* (Van Nostrand, Princeton, 1951) p. 447.
- ²⁴F. R. Kroeger and C. A. Swenson, J. Appl. Phys. **48**, 853 (1977).
- ²⁵K. Geschneider, Jr., Solid State Phys. **16**, 275 (1964).
- ²⁶T. W. Darling, A. Migliori, E. G. Moshopoulou, S. A. Trugman, J. J. Neumeier, J. L. Sarrao, A. R. Bishop, and J. D. Thompson, Phys. Rev. B **57**, 5093 (1998).
- ²⁷P. G. Radelli, M. Marezio, H. Y. Hwang, S.-W. Cheong, and B. Batlogg, Phys. Rev. B **54**, 8992 (1996).
- ²⁸J. L. García-Muñoz, M. Suaaidi, J. Fontcuberta, and J. Rodríguez-Carvajal, Phys. Rev. B **55**, 34 (1997).
- ²⁹M. F. Hundley, M. Hawley, R. H. Heffner, Q. X. Jia, J. J. Neumeier, J. Tesmer, J. D. Thompson, and X. D. Wu, Appl. Phys. Lett. **67**, 860 (1995).
- ³⁰G. Kwei, D. N. Argyiou, S. J. L. Billinge, A. C. Lawson, J. J. Neumeier, A. P. Ramirez, M. A. Subramanian, and J. D. Thompson, in *Magnetic Ultrathin Films, Multilayers and Surfaces—1997*, edited by D. D. Chambliss, J. G. Tobin, D. Kubinski, K. Barmak, W. J. M. de Jonge, T. Katayama, A. Schuhl, and P. Dederichs, MRS Symposia Proceedings No. 475 (Materials Research Society, Pittsburgh, 1997), p. 533.
- ³¹B. Sundqvist, Solid State Commun. **66**, 623 (1988); B. Sundqvist and B. M. Anderson, *ibid.* **76**, 1019 (1990).
- ³²T. Soumura, J. Phys. Soc. Jpn. **42**, 826 (1977).
- ³³J. L. Cohn, J. J. Neumeier, C. P. Popoviciu, K. J. McClellan, and Th. Leventouri, Phys. Rev. B **56**, R8495 (1997).